

Synthesis and Reactivity of Organosamarium Diarylpnictide Complexes: Cleavage Reactions of Group 15 E–E and E–C Bonds by Samarium(II)

William J. Evans,* John T. Leman, and Joseph W. Ziller

Department of Chemistry, University of California, Irvine, California 92717

Saeed I. Khan

Department of Chemistry and Biochemistry, University of California, Los Angeles, California 90024

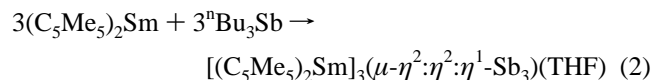
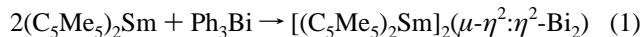
Received December 20, 1995[⊗]

(C₅Me₅)₂Sm (2 equiv) reacts with Ph₂EPh₂ to give (C₅Me₅)₂SmEPh₂ (E: P, **1**; As, **2**), while (C₅Me₅)₂Sm(THF)₂ (2 equiv) reacts with Ph₂EPh₂ to give (C₅Me₅)₂Sm(EPh₂)(THF) (E: P, **3**; As, **4**). **3** and **4** are also available from the reactions of **1** and **2** with THF. **3** and **4** undergo further reaction to produce the THF ring-opened products (C₅Me₅)₂Sm[O(CH₂)₄EPh₂](THF) (E: P, **5**; As, **6**). (C₅Me₅)₂Sm (4 equiv) reacts with Ph₂EPh₂ to give the mixed-valent (C₅Me₅)₂Sm(μ-EPh₂)Sm(C₅Me₅)₂ (E: P, **7**; As, **8**). These compounds are also available from the reaction of **1** and **2** with (C₅Me₅)₂Sm. The X-ray crystal structure of **2**, crystallized from hexanes (P2₁/n; a = 26.188(24) Å, b = 9.911(10) Å, c = 23.280(23) Å, β = 97.150(12)°, V = 5995(2) Å³, D_{calcd} = 1.488 Mg/m³; Z = 8; T = 156 K), revealed, in addition to a conventional seven-coordinate bent metallocene geometry with 2.698 Å Sm–C(C₅Me₅) and 2.970 Å Sm–As average distances, two very different Sm–As–C(Ph) angles, 74.2 and 118.7°. As a result, one phenyl group is closer to the metal (2.901 Å minimum Sm–C distance). **4**, crystallized from toluene (P2₁/n; a = 10.713(9) Å, b = 14.143(11) Å, c = 21.620(16) Å, β = 101.08(6)°, V = 3215(4) Å³, D_{calcd} = 1.492 Mg/m³; Z = 4; T = 163 K), and **6**, crystallized from hexanes (P2₁/n; a = 9.3958(16) Å, b = 22.245(3) Å, c = 17.931(3) Å, β = 96.497(11)°, V = 3724(1) Å³, D_{calcd} = 1.416 Mg/m³; Z = 4; T = 163 K), have conventional eight-coordinate, bent metallocene structures.

Introduction

Recent studies of the chemistry of the bent metallocene (C₅Me₅)₂Sm¹ with inorganic substrates including N₂,² BiPh₃,³ SbⁿBu₃,⁴ and elemental S, Se, and Te^{5,6} have revealed that this organometallic reagent offers opportunities to isolate and crystallographically characterize new and rare types of main group element compositions and structures. Hence, planar M₂N₂ and M₂Bi₂ units have been discovered in [(C₅Me₅)₂Sm]₂(μ-η²:η²-N₂)² and [(C₅Me₅)₂Sm]₂(μ-η²:η²-Bi₂),³ the (Sb₃)²⁻⁴ and (Se₃)⁴⁻⁶ ions have been structurally characterized for the first time, and facile routes to the relatively rare group 16 ions (S₃)²⁻, (Se₃)²⁻, and (Te₃)²⁻ have been found.⁵

In this study, we examine the generality of the reactions which formed the (Bi₂)²⁻ and (Sb₃)³⁻ ions in eqs 1 and 2. The



chemistry of (C₅Me₅)₂Sm and (C₅Me₅)₂Sm(THF)₂ with phos-

phorus and arsenic analogs is described as well as reactions of a series of alternative phenylbismuth precursors which were studied to learn more about reaction 1. These studies have revealed an unusual mixed-valent phosphorus compound and a system in which the stepwise coordination and ring opening of THF by an AsPh₂ unit can be documented.

Experimental Section

All manipulations described below employing (C₅Me₅)₂Sm and workup of subsequent reaction products were carried out under argon in an inert-atmosphere glovebox free of coordinating solvents. All other chemistry was performed under nitrogen with rigorous exclusion of air and water by using Schlenk, vacuum-line, and glovebox techniques. Physical measurements were obtained, solvents were purified, and (C₅Me₅)₂Sm¹ and (C₅Me₅)₂Sm(THF)₂⁷ were prepared as previously described.⁸ Ph₂PPPh₂,⁹ Ph₂AsAsPh₂,¹⁰ Ph₂SbSbPh₂,¹¹ and Ph₂BiBiPh₂,¹² were prepared by literature procedures. Ph₂BiCl was prepared by ligand redistribution between Ph₃Bi and BiCl₃ in a 2:1 molar ratio in refluxing toluene. Ph₂PH and Ph₂P(Al) employed in the synthesis of Ph₂PPPh₂ were distilled under vacuum before use. BiCl₃ was used as received. Ph₃P, Ph₃As, Ph₃Sb, and Ph₃Bi were recrystallized from absolute ethanol and dried under high vacuum.

(C₅Me₅)₂Sm(THF)_x/Ph₃E Reactions (x = 0, 2; E = P, As, Sb, Bi). The following general procedure was used to screen (C₅Me₅)₂Sm and (C₅Me₅)₂Sm(THF)₂ for reactivity toward the triphenylpnictides. A

[⊗] Abstract published in *Advance ACS Abstracts*, May 15, 1996.

- (1) Evans, W. J.; Hughes, L. A.; Hanusa, T. P. *J. Am. Chem. Soc.* **1984**, *106*, 4270. (b) Evans, W. J.; Hughes, L. A.; Hanusa, T. P. *Organometallics* **1986**, *5*, 1285.
- (2) Evans, W. J.; Ulibarri, T. A.; Ziller, J. W. *J. Am. Chem. Soc.* **1988**, *110*, 6877.
- (3) Evans, W. J.; Gonzales, S. L.; Ziller, J. W. *J. Am. Chem. Soc.* **1991**, *113*, 9880.
- (4) Evans, W. J.; Gonzales, S. L.; Ziller, J. W. *J. Chem. Soc., Chem. Commun.* **1992**, 1138.
- (5) Evans, W. J.; Rabe, G. W.; Ziller, J. W. *Inorg. Chem.* **1994**, *33*, 2719.
- (6) Evans, W. J.; Rabe, G. W.; Ziller, J. W.; Ansari, M. A. *Angew. Chem., Int. Ed. Engl.* **1994**, *33*, 210.

- (7) Evans, W. J.; Grate, J. W.; Choi, H. W.; Bloom, I.; Hunter, W. E.; Atwood, J. L. *J. Am. Chem. Soc.* **1985**, *107*, 941.
- (8) Evans, W. J.; Chamberlain, L. R.; Ulibarri, T. A.; Ziller, J. W. *J. Am. Chem. Soc.* **1988**, *110*, 6423.
- (9) Kuchen, W.; Buchwald, H. *Chem. Ber.* **1958**, *91*, 2871.
- (10) Busse, P. J.; Irgolic, K. J.; Dominguez, R. J. G. *J. Organomet. Chem.* **1974**, *81*, 45.
- (11) Hewertson, W.; Watson, H. R. *J. Chem. Soc.* **1962**, 1490.
- (12) Calderazzo, F.; Morvillo, A.; Pelizzi, G.; Poli, R. *J. Chem. Soc., Chem. Commun.* **1983**, 507.

small quantity (5–10 mg) of Ph₃E dissolved in 0.5 mL of C₆D₆ was treated dropwise with a solution of 2 equiv of the metallocene in an equal volume of the same solvent. The reaction mixtures were homogeneous in all cases. Aliquots were withdrawn and flame-sealed at atmospheric pressure in 5 mm NMR tubes.

(C₅Me₅)₂Sm(PPh₂), 1. A solution of (C₅Me₅)₂Sm (100.5 mg, 0.239 mmol) in toluene (3 mL) was added dropwise to a stirred solution of Ph₂PPPPh₂ (44.1 mg, 0.119 mmol) in toluene (3 mL). The deep-green color of the (C₅Me₅)₂Sm solution was quenched immediately to a pale brown color which increased in intensity as the addition progressed. After 15 min of stirring, the solvent was removed in vacuo to give a dark brown oil, which was triturated with hexanes (1 mL). The resultant brown solid was dried under vacuum to give pure **1** (132 mg, 90%). Anal. Calcd for C₃₂H₄₀SmP: C, 63.42; H, 6.65; Sm, 24.81; P, 5.11. Found: C, 63.20; H, 6.77; Sm, 25.10; P, 5.22. Isopiestic molecular weight (0.057 M in C₆H₆): calcd for C₃₂H₄₀SmP, 606; found, 560. ¹H NMR (C₆D₆, 300 MHz, 25 °C): δ 5.82 (t, *J* = 7.3 Hz, 2H, Ph *p*-H), 4.54 (br "t", Δ*v*_{1/2} = 10 Hz, 4H, Ph *m*-H), 3.43 (br d, Δ*v*_{1/2} = 20 Hz, 4H, Ph *o*-H), 0.54 (s, 30H, C₅Me₅). ¹³C NMR (C₆D₆, 25 °C): δ 155.5, 120.5, 118.1 (C₆H₅), 118.7 (C₅Me₅), 19.6 (C₅Me₅). Magnetic susceptibility: χ_M^{293K} = 425 × 10⁻⁶ cgsu; μ_{eff} = 1.0 μ_B.

(C₅Me₅)₂Sm(AsPh₂), 2. As described above for **1**, (C₅Me₅)₂Sm (96.5 mg, 0.229 mmol) and Ph₂AsAsPh₂ (52.5 mg, 0.114 mmol) were combined in toluene (5 mL). Removal of the solvent under vacuum gave a brown powder which was pure by ¹H NMR spectroscopy. Cooling a warm saturated hexane solution to -36 °C gave dark brown plates of **2** (92 mg, 65%) suitable for X-ray crystallography. Anal. Calcd for C₃₂H₄₀SmAs: C, 59.14; H, 6.20; Sm, 23.13; As, 11.53. Found: C, 58.91; H, 6.17; Sm, 23.40; As, 11.35. Isopiestic molecular weight (0.038 M in C₆H₆): calcd for C₃₂H₄₀SmAs, 650; found, 624. ¹H NMR (C₆D₆, 300 MHz, 25 °C): δ 5.84 (t, *J* = 7.3 Hz, 2H, Ph *p*-H), 4.68 (br "t", Δ*v*_{1/2} = 18 Hz, 4H, Ph *m*-H), 3.75 (br d, Δ*v*_{1/2} = 18 Hz, 4H, Ph *o*-H), 0.53 (s, 30H, C₅Me₅). ¹³C NMR (C₆D₆, 25 °C): δ 157.1, 134.8, 122.1, 121.8 (C₆H₅), 118.7 (C₅Me₅), 19.4 (C₅Me₅). Magnetic susceptibility: χ_M^{293K} = 437 × 10⁻⁶ cgsu; μ_{eff} = 1.0 μ_B.

(C₅Me₅)₂Sm(PPh₂)(THF), 3. As described above for **1**, (C₅Me₅)₂Sm(THF)₂ (173.6 mg, 0.307 mmol) and Ph₂PPPPh₂ (56.8 mg, 0.152 mmol) were combined in toluene (5 mL). A dark brown color developed immediately, and after 15 min the solvent was removed under vacuum to give a brown oil. Trituration with hexanes (2 mL), removal of the solvent via pipet, and vacuum-drying gave a green-brown solid, **3** (218 mg, 95%). Anal. Calcd for C₃₆H₄₈SmOP: Sm, 22.17. Found: Sm, 21.7. ¹H NMR (C₆D₆ + 1 equiv THF, ¹³C 300 MHz, 25 °C): δ 6.94 (t, *J* = 7.4 Hz, 2H, Ph *p*-H), 6.59 ("t", *J* = 7.2 Hz, 4H, Ph *m*-H), 5.82 (d, *J* = 7.2 Hz, 4H, Ph *o*-H), 1.20 (s, 30H, C₅Me₅). ¹³C NMR (C₆D₆, 25 °C): δ 148.4, 133.2 (d, *J*_{P-C} = 22 Hz), 128.2, 121.8 (C₆H₅), 117.1 (C₅Me₅), 65.7 (br, α-C, THF), 21.4 (br, β-C, THF), 18.5 (C₅Me₅). Magnetic susceptibility: χ_M^{293K} = 419 × 10⁻⁶ cgsu; μ_{eff} = 1.0 μ_B.

(C₅Me₅)₂Sm(AsPh₂)(THF), 4. (C₅Me₅)₂Sm(THF)₂ (143.5 mg, 0.254 mmol) and Ph₂AsAsPh₂ (58.2 mg, 0.127 mmol) were combined in toluene (5 mL) as described for **3**. Trituration with hexanes (2 mL), removal of the solvent, and vacuum-drying gave a green-brown solid, **4** (140 mg, 77%). Anal. Calcd for C₃₆H₄₈SmAsO: Sm, 20.82. Found: Sm, 20.20. ¹H NMR (C₆D₆ + 1 equiv THF, ¹³C 300 MHz, 25 °C): δ 6.92 (t, *J* = 7.2 Hz, 2H, Ph *p*-H), 6.57 ("t", *J* = 7.4 Hz, 4H, Ph *m*-H), 5.64 (d, *J* = 7.4 Hz, 4H, Ph *o*-H), 1.22 (s, 30H, C₅Me₅). ¹³C NMR (C₆D₆, 25 °C): δ 149.4, 131.2, 127.8, 122.7 (C₆H₅), 117.2 (C₅Me₅), 65.4 (br, α-C, THF), 21.3 (br, β-C, THF), 18.3 (C₅Me₅). Magnetic susceptibility: χ_M^{293K} = 354 × 10⁻⁶ cgsu; μ_{eff} = 0.9 μ_B.

(C₅Me₅)₂Sm[O(CH₂)₄PPh₂](THF), 5. A solution of **3**, prepared as above from (C₅Me₅)₂Sm(THF)₂ (190 mg, 0.34 mmol) and Ph₂PPPPh₂ (62.1 mg, 0.17 mmol) in THF (5 mL) was placed in a 50 mL, thick-walled glass reaction tube equipped with a Teflon high-vacuum stopcock. The solution was degassed by three freeze-pump-thaw

cycles on a high-vacuum line, left under vacuum, and placed in an oil bath at 65 °C. After 60 h, the solution had changed from its initial dark brown color to yellow. The THF was removed under vacuum, and the resultant yellow oil was taken up in hexane (1 mL), centrifuged to remove a small amount of insolubles, and then cooled to -40 °C. Yellow crystals of **5** (178 mg, 70%) were isolated by decantation from the mother liquor followed by vacuum-drying. Anal. Calcd for C₄₀H₅₆SmPO₂: C, 64.04; H, 7.52; Sm, 20.04. Found: C, 55.77; H, 6.73; Sm, 21.28. ¹H NMR (C₆D₆, 300 MHz, 25 °C): δ 7.61 ("t", *J* = 6.9 Hz, 4H, Ph *o*-H), 7.10 (mult, 4H, Ph *m*-H), 7.04 (mult, 2H, Ph *p*-H), 5.50 (br mult, Δ*v*_{1/2} = 17 Hz, 2H, CH₂), 4.05 (br mult, Δ*v*_{1/2} = 22 Hz, 2H, CH₂), 2.77 (br mult, Δ*v*_{1/2} = 14 Hz, 4H, CH₂), 1.40 (s, 30H, C₅Me₅), -2.29 (br s, Δ*v*_{1/2} = 60 Hz, 4H, THF), -3.59 (br s, Δ*v*_{1/2} = 140 Hz, 4H, THF). ¹³C NMR (C₆D₆, 25 °C): δ 140.2 (d, *J*_{P-C} = 15 Hz, C₆H₅), 133.5 (C₆H₅), 133.3 (d, *J*_{P-C} = 18 Hz, C₆H₅), 128.6 (mult, C₆H₅), 113.5 (C₅Me₅), 74.0 [O(CH₂)₄PPh₂], 60.8 (br, α-C, THF), 37.8 (d, *J*_{P-C} = 12 Hz, [O(CH₂)₄PPh₂]), 29.6 (d, *J*_{P-C} = 12 Hz, [O(CH₂)₄PPh₂]), 24.8 (d, *J*_{P-C} = 16 Hz, [O(CH₂)₄PPh₂]), 19.4 (br, β-C, THF), 17.9 (C₅Me₅). Magnetic susceptibility: χ_M^{293K} = 537 × 10⁻⁶ cgsu; μ_{eff} = 1.1 μ_B.

(C₅Me₅)₂Sm[O(CH₂)₄AsPh₂](THF), 6. A solution of **4**, prepared as above from (C₅Me₅)₂Sm(THF)₂ (75.4 mg, 0.133 mmol) and Ph₂AsAsPh₂ (30.5 mg, 0.067 mmol) in THF (5 mL) was placed in a 50 mL, thick-walled glass reaction tube equipped with a Teflon high-vacuum stopcock. The solution was degassed by three freeze-pump-thaw cycles on a high-vacuum line, left under vacuum, and placed in an oil bath at 65 °C. After 20 h, the solution had undergone a change from its initial dark brown color to yellow, which was similar to that seen for the conversion of **3** to **5** above. The THF was removed under vacuum, and the resultant yellow oil was taken up in hexane (1 mL), centrifuged to remove a small amount of insolubles, and then cooled to -40 °C. Yellow crystals of **6** (83 mg, 79%) were isolated by decantation from the mother liquor, followed by vacuum-drying. Crystals for the X-ray diffraction study were grown from a dilute solution of **4** in hexane over an extended period of time. Anal. Calcd for C₄₀H₅₆SmAsO₂: C, 60.50; H, 7.11; Sm, 18.93. Found: C, 58.63; H, 7.10; Sm, 18.88. ¹H NMR (C₆D₆, 300 MHz, 25 °C): δ 7.61 (d, *J* = 7.0 Hz, 4H, Ph *o*-H), 7.11 ("t", *J* = 7.8 Hz, 4H, Ph *m*-H), 7.04 (t, *J* = 7.1 Hz, 2H, Ph *p*-H), 5.51 (br mult, Δ*v*_{1/2} = 15 Hz, 2H, CH₂), 4.05 (br mult, Δ*v*_{1/2} = 15 Hz, 2H, CH₂), 2.77 (br mult, Δ*v*_{1/2} = 15 Hz, 2H, CH₂), 2.75 (broad mult, Δ*v*_{1/2} = 15 Hz, 2H, CH₂), 1.40 (s, 30H, C₅Me₅), -2.38 (br s, Δ*v*_{1/2} = 40 Hz, 4H, THF), -3.66 (br s, Δ*v*_{1/2} = 75 Hz, 4H, THF). ¹³C NMR (C₆D₆, 25 °C): δ 141.8, 133.5, 131.6, 128.8 (C₆H₅), 113.5 (C₅Me₅), 74.0 [O(CH₂)₄AsPh₂], 61.3 (br, α-C, THF), 38.3, 29.5, 25.2 [O(CH₂)₄AsPh₂], 19.8 (br, β-C, THF), 17.9 (C₅Me₅). Magnetic susceptibility: χ_M^{293K} = 379 × 10⁻⁶ cgsu; μ_{eff} = 0.95 μ_B.

(C₅Me₅)₂Sm(μ-PPh₂)Sm(C₅Me₅), 7. A solution of Ph₂PPPPh₂ (23.7 mg, 0.064 mmol) in toluene (3 mL) was treated with a solution of (C₅Me₅)₂Sm (107.9 mg, 0.256 mmol) in toluene (3 mL) and isolated as for **1** above. Anal. Calcd for C₅₂H₇₀Sm₂P: C, 60.82; H, 6.87; Sm, 29.29; P, 3.02. Found: C, 60.45; H, 6.72; Sm, 29.65; P, 3.24. ¹H NMR (C₆D₆, 300 MHz, 25 °C, concentration dependent, 5.6 mM): δ 6.13 (t, *J* = 7.1 Hz, 1H, Ph *p*-H), 5.20 (br mult, Δ*v*_{1/2} = 20 Hz, 2H, Ph *m*-H), 3.73 (br mult, Δ*v*_{1/2} = 20 Hz, 2H, Ph *o*-H), 0.80 (s, 30H, C₅Me₅). ¹³C NMR (C₆D₆, 25 °C): δ 180.6, 133.3, 128.5, 121.0 (C₆H₅), 57.8 (C₅Me₅), 17.3 (C₅Me₅). Magnetic susceptibility: χ_M^{293K} = 2560 × 10⁻⁶ cgsu; μ_{eff} = 2.45 μ_B.

Isolated **1** (39.0 mg, 0.065 mmol) was reacted in a similar fashion with (C₅Me₅)₂Sm (28.7 mg, 0.068 mmol) in toluene (3 mL). The ¹H NMR spectrum of the resulting brown solid corresponded closely to that for (C₅Me₅)₂Sm(μ-PPh₂)Sm(C₅Me₅) above. ¹H NMR (C₆D₆, 300 MHz, 25 °C, concentration dependent, 5.6 mM): δ 6.11 (t, 1H, Ph *p*-H), 5.15 (br "t", 2H, Ph *m*-H), 3.70 (br d, 2H, Ph *o*-H), 0.79 (s, 30H, C₅Me₅).

(C₅Me₅)₂Sm(μ-AsPh₂)Sm(C₅Me₅), 8. Ph₂AsAsPh₂ (5.0 mg, 0.011 mmol) and (C₅Me₅)₂Sm (18.4 mg, 0.044 mmol) were combined in C₆D₆ (1.20 mL), and the NMR spectrum was measured immediately. ¹H NMR (C₆D₆, 300 MHz, 25 °C, concentration dependent, 18 mM): δ 8.40 (br s, Δ*v*_{1/2} = 30 Hz, 2H, C₆H₅), 7.68 (s, Δ*v*_{1/2} = 20 Hz, 1H, Ph *p*-H), 5.49 (br s, Δ*v*_{1/2} = 30 Hz, 2H, C₆H₅), 1.00 (s, 30H, C₅Me₅).

Isolated **2** (13.5 mg, 0.021 mmol) and (C₅Me₅)₂Sm (8.9 mg, 0.021

(13) In the absence of additional THF, the NMR spectrum of **3** is highly dependent on the extent of drying of the compound and the amount of THF present. Chemical shifts are observed in the following ranges: 6.71–6.94 (Ph *p*-H), 6.16–6.59 (Ph *m*-H), 5.33–5.82 (Ph *o*-H), and 1.08–1.20 (C₅Me₅) ppm.

(14) Compound **4** is like **3**. ¹³C Chemical shifts are observed in the following ranges: 6.81–6.92 (Ph *p*-H), 6.37–6.57 (Ph *m*-H), 5.44–5.64 (Ph *o*-H), and 1.15–1.22 (C₅Me₅) ppm.

Table 1. Crystal Data and Experimental Details for the X-ray Diffraction Studies of **2**, **4**, and **6**

	(C ₅ Me ₅) ₂ SmAsPh ₂ · ¹ / ₄ C ₆ H ₁₄ (2· ¹ / ₄ C ₆ H ₁₄)	(C ₅ Me ₅) ₂ SmAsPh ₂ (THF) (4)	(C ₅ Me ₅) ₂ SmO(CH ₂) ₄ AsPh ₂ (THF) (6)
empirical formula	C ₃₂ H ₄₀ SmAs· ¹ / ₄ C ₆ H ₁₄	C ₃₆ H ₄₈ SmAsO	C ₄₀ H ₅₆ SmAsO ₂
fw	671.45	722.0	794.1
temp (K)	156	163	163
crystal system	monoclinic	monoclinic	monoclinic
space group	P ₂ ₁ /n	P ₂ ₁ /n	P ₂ ₁ /n
a (Å)	26.188(24)	10.713(9)	9.3958(16)
b (Å)	9.911(10)	14.143(11)	22.245(3)
c (Å)	23.280(23)	21.620(16)	17.931(3)
β (deg)	97.150(12)	101.08(6)	96.497(11)
V (Å ³)	5995(2)	3215(4)	3724(1)
Z	8	4	4
D _{calcd} (Mg/m ³)	1.488	1.429	1.416
diffractometer	Picker (Crystal Logic)	Siemens P3	Siemens P3
radiation (λ (Å))	Mo Kα (0.710 730)	Mo Kα (0.710 730)	Mo Kα (0.710 730)
scan type	θ-2θ	ω	θ-2θ
2θ range (deg)	1.0-45.0	4.0-40.0	4.0-45.0
μ(Mo Kα) (mm ⁻¹)	3.080	2.874	2.490
abs cor	semiempirical (ψ-scan method)	none	semiempirical (ψ-scan method)
R _F ^a	0.068	0.080	0.045
R _{wF} ^a	0.076	0.103	0.047

$$^a R_F = \sum ||F_o| - |F_c|| / \sum |F_o|; R_{wF} = \sum w(|F_o| - |F_c|)^2 / \sum w|F_o|^2.$$

mmol) were combined in C₆D₆ (1.13 mL) and analyzed immediately. The ¹H NMR spectrum of the resulting brown solution was nearly identical to that of (C₅Me₅)₂Sm(μ-AsPh₂)Sm(C₅Me₅)₂ above. ¹H NMR (C₆D₆, 300 MHz, 25 °C, concentration dependent, 19 mM): δ 8.47 (br s, Δν_{1/2} = 30 Hz, 2H, C₆H₅), 7.71 (br s, Δν_{1/2} = 20 Hz, 1H, Ph p-H), 5.53 (br s, Δν_{1/2} = 30 Hz, 2H, C₆H₅), 0.99 (s, 30H, C₅Me₅).

Reaction of (C₅Me₅)₂Sm(μ-PPH₂)Sm(C₅Me₅)₂, **7, with Ph₂PPPPh₂.** Ph₂PPPPh₂ (0.8 mg, 0.002 mmol) and (C₅Me₅)₂Sm(μ-PPH₂)Sm(C₅Me₅)₂ (3.9 mg, 0.004 mmol) were combined in C₆D₆ (≈0.5 mL) and allowed to react for 5 min, producing a dark brown solution. The solution was examined by ¹H NMR spectroscopy, which showed complete reaction to form (C₅Me₅)₂SmPPH₂, **1**.

X-ray Data Collection, Structure Determination, and Refinement for 2. A deep red, irregularly-shaped crystal of **2** of approximate dimensions 0.30 × 0.26 × 0.20 mm was coated with Paratone oil, mounted on the tip of a glass fiber, and transferred to the 156 K nitrogen cold stream of a modified four-circle Picker diffractometer equipped with a monochromatized Mo X-ray source. Accurate cell dimensions and the crystal orientation matrix were determined by a least-squares fit of the setting angles of 20 reflections in the range 12 < 2θ < 20°. Intensity data were collected by the θ-2θ method using a scan speed of 3.0°/min up to a maximum 2θ = 45°. Three intense reflections were monitored after every 97 reflections collected and showed no significant variation. The intensities of 7856 reflections were measured, of which 4109 had |F_o| > 6.0σ(|F_o|) and were considered observed. Data were corrected for Lorentz and polarization effects, and an empirical absorption correction based on ψ-scans was applied. A summary of crystallographic data is included in Table 1.

The structure was solved by Patterson methods and expanded by Fourier techniques in the monoclinic space group P₂₁/n.¹⁵ Hydrogen atoms were included in calculated positions and were constrained to ride upon the appropriate carbon atoms. For methyl groups, at least one of the hydrogen atoms was located from the difference-Fourier map. A disordered solvent molecule, presumably n-hexane, was located close to the inversion center, but could not be refined satisfactorily. The three strongest peaks from the difference map were arbitrarily assigned as carbon atoms and were not refined. A total of 293 parameters with Sm and As anisotropic and all other non-hydrogens atoms isotropic were refined using full-matrix least-squares techniques. Refinement converged at R_F = 6.8%, R_{wF} = 7.6%. An anomalous dispersion correction was applied to all non-hydrogen atoms.¹⁶ The final difference electron density map showed some residual electron density (ρ(max) = 2.45 e Å⁻³) close to the disordered solvent molecule; the rest of the map was featureless.

X-ray Data Collection, Structure Determination, and Refinement for 4 and 6. A dark orange crystal of **4** of approximate dimensions 0.17 × 0.20 × 0.38 mm was oil-mounted¹⁷ on a glass fiber and transferred to a Siemens P3 diffractometer. The determinations of Laue symmetry, crystal class, unit cell parameters, and the crystal's orientation matrix were carried out by previously described methods similar to those of Churchill.¹⁸ Intensity data were collected at 163 K using an ω-scan technique with Mo Kα radiation under the conditions described in Table 1. All 3393 data were corrected for Lorentz and polarization effects and were placed on an approximately absolute scale. Any reflection with I(net) < 0 was assigned the value |F_o| = 0. The diffraction symmetry was 2/m with systematic absences 0k0 for k = 2n + 1 and h0l for h + l = 2n + 1. The centrosymmetric monoclinic space group P₂₁/n [C_{2h}⁵; No. 14] is therefore uniquely defined.

All crystallographic calculations were carried out using either our locally modified version of the UCLA Crystallographic Computing Package¹⁵ or the SHELXTL PLUS program set.¹⁹ The analytical scattering factors for neutral atoms were used throughout the analysis²⁰ both the real (Δf') and imaginary (iΔf'') components of anomalous dispersion were included. The quantity minimized during least-squares analysis was Σw(|F_o| - |F_c|)² where w⁻¹ = σ²(|F_o|) + 0.0020(|F_o|)².

The structure was solved by direct methods and refined by full-matrix least-squares techniques. Hydrogen atoms were included using a riding model with d(C-H) = 0.96 Å and U(iso) = 0.08 Å². Refinement of positional and thermal parameters led to convergence with R_F = 8.0%, R_{wF} = 10.3%, and GOF = 1.61 for 167 variables refined against those 2232 data with |F_o| > 4.0σ(|F_o|). A final difference-Fourier map was devoid of significant features; ρ(max) = 2.10 e Å⁻³. The crystal decomposed after data were collected to a 2θ(max) of 40.0°. It was therefore not possible to apply an absorption correction since our standard practice is to measure ψ scans at the conclusion of data collection.

A pale yellow crystal of **6** of approximate dimensions 0.13 × 0.33 × 0.36 mm was handled as described above for **4**. Intensity data were collected at 163 K. Details appear in Table 1. All 5410 data were

(15) UCLA Crystallographic Computing Package, University of California, Los Angeles, 1981; C. Strouse, personal communication.

(16) *International Tables for X-Ray Crystallography*; Kynoch: Birmingham, England, 1974; Vol. IV.

(17) The crystal was immersed in a lube-oil additive, which allowed for manipulation on the bench top and prevented decomposition due to air or moisture. The crystal was secured to a glass fiber (the oil acts as the adhesive) which was attached to an elongated brass mounting pin. Further details appear in: Hope, H. *Experimental Organometallic Chemistry: A Practicum in Synthesis and Characterization*; Wayda, A. L., Darensbourg, M. Y., Eds.; ACS Symposium Series 357; American Chemical Society: Washington, DC, 1987.

(18) Churchill, M. R.; Lashewycz, R. A.; Rotella, F. J. *Inorg. Chem.* **1977**, *16*, 265.

(19) Sheldrick, G. *SHELXTL PLUS program set*; Siemens Analytical X-Ray Instruments, Inc.: Madison, WI, 1990.

(20) *International Tables for X-Ray Crystallography*; Kluwer Academic Publishers: Dordrecht, The Netherlands, 1992; Vol. C.

corrected for absorption and for Lorentz and polarization effects and placed on an approximately absolute scale. The diffraction symmetry was $2/m$ with systematic absences $0k0$ for $k = 2n + 1$ and $h0l$ for $h + l = 2n + 1$. The centrosymmetric monoclinic space group $P2_1/n$ [C_{2h}^5 ; No. 14] is therefore uniquely defined. All crystallographic calculations were carried out as described above for **4**. The quantity minimized during least-squares analysis was $\sum w(|F_o| - |F_c|)^2$ where $w^{-1} = \sigma^2(|F_o|) + 0.0004(|F_o|)^2$.

The structure was solved by direct methods and refined by full-matrix least-squares techniques. Hydrogen atoms were included using a riding model with $d(C-H) = 0.96 \text{ \AA}$ and $U(\text{iso}) = 0.08 \text{ \AA}^2$. Refinement of positional and thermal parameters led to convergence with $R_F = 4.5\%$, $R_{wF} = 4.7\%$, and $\text{GOF} = 1.42$ for 397 variables refined against those 4053 data with $|F_o| > 3.0\sigma(|F_o|)$. A final difference-Fourier map yielded $\rho(\text{max}) = 0.81 \text{ e \AA}^{-3}$.

Results and Discussion

Reactions of $(C_5Me_5)_2Sm(THF)_x$ with Ph_3E ($x = 0, 2$; $E = P, As, Sb, Bi$). The reactivity of $(C_5Me_5)_2Sm$ and $(C_5Me_5)_2Sm(THF)_2$ with the group 15 triphenyl compounds, Ph_3E , was surveyed as shown in Table 2. Each system was periodically monitored by NMR until no further changes in the spectrum occurred. As expected, $(C_5Me_5)_2Sm$ is more reactive than $(C_5Me_5)_2Sm(THF)_2$ and cleavage of the E–C bonds is more facile for the heavier congeners in group 15.

Table 2. Summary of Reactivity of $(C_5Me_5)_2Sm(THF)_x$ with Triphenylpnictides

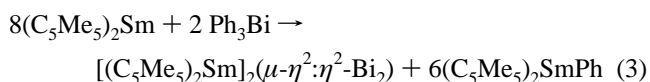
compd	Ph_3P	Ph_3As	Ph_3Sb	Ph_3Bi
$(C_5Me_5)_2Sm$ adduct formn	no react	E–C cleavage	E–C cleavage	E–C cleavage
$(C_5Me_5)_2Sm(THF)_2$ no react	no react	no react	E–C cleavage	E–C cleavage

In the experiments with $(C_5Me_5)_2Sm(THF)_2$ and Ph_3P , Ph_3As , and Ph_3Sb , no significant perturbation of the Ph_3E resonances from their positions in the free ligands was observed and the low-field resonance characteristic for coordinated THF remained.²¹ Apparently, none of these group 15 triphenyl complexes are sufficiently Lewis basic to displace the THF. In contrast, addition of base-free $(C_5Me_5)_2Sm$ to Ph_3P causes the multiplets in free Ph_3P at 7.38 and 7.03 ppm (2:3 ratio) to change to a series of triplet-like peaks at 7.80, 7.20, and 7.07 ppm in a ratio of 2:2:1. Selective homonuclear spin-decoupling experiments confirmed these peaks as arising from the *o*-, *m*-, and *p*-protons, respectively. Coordination of the phosphine perturbs the *o*-H resonances the most and removes the near-degeneracy in chemical shift of the *m*- and *p*-protons in the free ligand.

In order to probe the stoichiometry of this system, portions of $(C_5Me_5)_2Sm$ were added to a solution of Ph_3P up to the 2:1 ratio employed above. No further change in the NMR spectrum of the system occurred after the Sm:P ratio exceeded unity, which indicates formation of a 1:1 metal–ligand complex. Similar shifts were not observed between $(C_5Me_5)_2Sm$ and Ph_3As . Formation of a phosphine complex of the very electrophilic $(C_5Me_5)_2Sm$ ^{2,22} is not unexpected, given the crystallographically established structures of both divalent and trivalent lanthanide phosphine complexes such as $Yb[N(SiMe_3)_2]_2(Me_2PCH_2CH_2PMe_2)$,²³ $(C_5Me_5)_2YbCl(Me_2PCH_2PMe_2)$,²⁴ $La[TeSi(SiMe_3)_3]_3(Me_2PCH_2CH_2PMe_2)_2$,²⁵ $(MeC_5H_4)_3Ce(PMe_3)$,²⁶ and $Nd[OCH(PMe_2)CH(t-C_4H_9)_2]_3$.²⁷

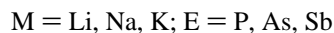
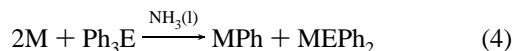
No evidence for a stable 1:1 acid base adduct, $(C_5Me_5)_2Sm(EPh_3)$, was found in reactions of $(C_5Me_5)_2Sm$ with Ph_3Sb and Ph_3Bi , however. Instead, E–C cleavage reactions occur. In the bismuth case, the reaction is immediate and $[(C_5Me_5)_2Sm]_2(\mu-\eta^2:\eta^2-Bi_2)$ and $(C_5Me_5)_2SmPh$ are formed. For Sb, the reaction is slower. The C_5Me_5 resonance of the starting material disappears over a 1–2 day period, and $(C_5Me_5)_2SmPh$ can be identified by 1H NMR in the product mixture obtained. No clear evidence for products such as $[(C_5Me_5)_2Sm]_3(\mu-\eta^2:\eta^2:\eta^1-Sb_3)(THF)$ or $[(C_5Me_5)_2Sm]_2(\mu-\eta^2:\eta^2-Sb_2)$ was found. Ph_3Bi also reacts with $(C_5Me_5)_2Sm(THF)_2$ to give $(C_5Me_5)_2SmPh(THF)$, but no other organosamarium products were identifiable.

As previously reported,³ the reaction of 2 equiv of $(C_5Me_5)_2Sm$ with 1 equiv of Ph_3Bi forms $[(C_5Me_5)_2Sm]_2(\mu-\eta^2:\eta^2-Bi_2)$ and $(C_5Me_5)_2SmPh$. Further investigation of this reaction shows that not all of the Ph_3Bi is consumed with this stoichiometry and the complicated mixture of products formed in the 2:1 reaction can be avoided if a 4:1 Sm:Bi ratio is used. As shown in eq 3, a 4:1 ratio leads to complete consumption of both



reactants and clean formation of only $[(C_5Me_5)_2Sm]_2(\mu-\eta^2:\eta^2-Bi_2)$ and $(C_5Me_5)_2SmPh$.

Cleavage of E–C bonds has previously been observed with group 15 compounds in reactions with alkali metals. For example, Gilman et al.²⁸ established that alkali metals in liquid ammonia or THF easily cleave the E–C bond in Ph_3E compounds as shown in eq 4. When reactions with excess alkali



metal in liquid ammonia were quenched with NH_4Cl , the products were Ph_2EH and benzene for P, As, and Sb.²⁹ The corresponding reduction of Ph_3Bi was different, however, in that only benzene (3 equiv) was observed.

E–C cleavage in reactions of $(C_5Me_5)_2Sm(THF)_2$ and $(C_5Me_5)_2Sm$ with Ph_3E is therefore reasonable, since parallels between the reactions of alkali metals and these bent metallocenes have been previously noted in reactions with substrates as diverse as CO ³⁰ and anthracene.³¹ The $(C_5Me_5)_2Sm(THF)_x$ reagents differ from alkali metals, however, because they are more soluble and the presence of $(C_5Me_5)_2Sm$ units allows for the assembly and isolation of reduced products either not accessible or unstable with alkali metals. Hence, $[(C_5Me_5)_2Sm]_2(\mu-\eta^2:\eta^2-Bi_2)$, rather than metallic bismuth or insoluble, uncharacterized alkali metal bismuthides, is isolated in reaction 1. Since Bi–C bonds are the weakest in the EPh_3 series,³² it is reasonable that Ph_3Bi is the most likely to undergo E–C cleavage and form polyelement anions (Zintl ions).

Reactions of $(C_5Me_5)_2Sm$ with Ph_2PPPPh_2 and $Ph_2AsAsPh_2$: Formation of $(C_5Me_5)_2Sm(EPh_2)$ ($E = P, As$). Since the Ph_3E compounds of the lighter congeners in group 15 did not undergo E–C cleavage to form homopolyatomic anions, other precursors to these anions were sought. The

(21) Evans, W. J.; Bloom, I.; Hunter, W. E.; Atwood, J. L. *Organometallics* **1985**, *4*, 112.

(22) Evans, W. J. *Polyhedron* **1987**, *6*, 803.

(23) Tilley, T. D.; Andersen, R. A.; Zalkin, A. *J. Am. Chem. Soc.* **1982**, *104*, 3725.

(24) Tilley, T. D.; Andersen, R. A.; Zalkin, A. *Inorg. Chem.* **1983**, *22*, 856.

(25) Cary, D. R.; Arnold, J. *J. Am. Chem. Soc.* **1993**, *115*, 2520.

(26) Stults, S.; Zalkin, A. *Acta Crystallogr., Sect. C* **1987**, *43*, 430.

(27) Hitchcock, P. B.; Lappert, M. F.; MacKinnon, I. A. *J. Chem. Soc., Chem. Commun.* **1988**, 1557.

(28) Gilman, H.; Wittenberg, D. *J. Org. Chem.* **1958**, *23*, 1063.

(29) Rossi, R. A.; Bunnett, J. F. *J. Am. Chem. Soc.* **1974**, *96*, 112.

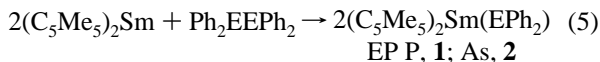
(30) Evans, W. J.; Grate, J. W.; Hughes, L. A.; Zhang, H.; Atwood, J. L. *J. Am. Chem. Soc.* **1985**, *107*, 3728.

(31) Evans, W. J.; Gonzales, S. L.; Ziller, J. W. *J. Am. Chem. Soc.* **1994**, *116*, 2600.

(32) Steele, W. V. *J. Chem. Thermodyn.* **1979**, *11*, 187.

Ph₂EPh₂ compounds were attractive, since they contained one less E–C(phenyl) bond compared to Ph₃E. The availability of Ph₂EPh₂ for E = P, As, Sb, and Bi also allows for a comparison of reactivity in a homologous series, as was done for Ph₃E.

(C₅Me₅)₂Sm (2 equiv) reacts quickly and quantitatively with Ph₂PPPPh₂ and Ph₂AsAsPh₂ to give the Sm(III) phosphide and arsenide compounds **1** and **2**, respectively, as shown in eq 5.



Both compounds are dark brown crystalline solids which are soluble in hexane and stable in both the solid state and solution at room temperature under an inert atmosphere. These compounds are hydrolytically sensitive and decompose to [(C₅Me₅)₂Sm]₂(μ-O)³³ and Ph₂EH when exposed to moisture. The ¹H NMR spectra of **1** and **2** show a single sharp resonance for the C₅Me₅ ligand and a single A₂B₂C monosubstituted phenyl ring pattern, arising from the Ph₂E– group. The equivalence of the two phenyl rings dictates either that the Ph₂E– ligand is in a highly symmetrical environment or that there is free rotation about the E–Ph bonds in solution. For the former case, a symmetrical bridging μ–EPh₂ mode of coordination, such as that seen in (C₅H₅)₂Lu(μ–EPh₂)₂Li(TMED) (E = P,³⁴ As³⁵), is consistent with the NMR data. However, previous studies have shown that [(C₅Me₅)₂Sm(μ–Z)]₂ complexes where Z is a large anionic ligand are likely to be too sterically crowded to form simple bridged dimers.³⁶ Consistent with this supposition, solution molecular weight measurements show **1** and **2** to be monomeric in benzene, which implies a terminal mode of coordination and formally seven-coordinate structures. This is consistent with the spectroscopic and analytical data reported for the related species (MeC₅H₄)₂Sm(PPh₂)³⁷ and (C₅Me₅)₂Sm(PEt₂).³⁸

Since all phenyl resonances appear at unusually high field for aromatic protons (3–6 ppm range) and only the lowest field triplets in the ¹H NMR spectra, assigned to the *p*-H are well-resolved, additional weak Sm⋯H–C interactions may exist in solution which serve to increase the effective coordination number. The other resonances for the *o*- and *m*-protons are broadened and may be indicative of further metal–ligand interaction. This is supported by the solid state structure described below for **2** and by the fact that upon addition of THF to these complexes all the resonances become well resolved and move downfield to a more normal range for aromatic protons. A similar situation is observed for the benzyl and phenyl complexes (C₅Me₅)₂SmCH₂Ph³⁹ and (C₅Me₅)₂SmPh.²¹ For the unsolvated complexes the aryl *o*-H and *m*-H resonances are at high field and are poorly resolved or otherwise unobservable. Addition of THF also sharpens these resonances and causes them to move to the normal aromatic region.

Reactions of (C₅Me₅)₂Sm(THF)₂ with Ph₂PPPPh₂ and Ph₂AsAsPh₂: Formation of (C₅Me₅)₂Sm(EPh₂)(THF) Species

(33) Evans, W. J.; Grate, J. W.; Bloom, I.; Hunter, W. E.; Atwood, J. L. *J. Am. Chem. Soc.* **1985**, *107*, 405.

(34) Schumann, H.; Palamidis, E.; Schmid, G.; Boese, R. *Angew. Chem., Int. Ed. Engl.* **1986**, *25*, 718.

(35) Schumann, H.; Palamidis, E.; Loebel, J.; Pickhardt, J. *Organometallics* **1988**, *7*, 1008.

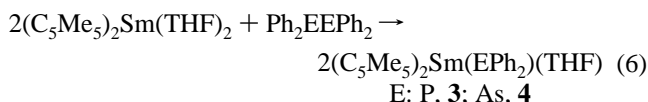
(36) (a) Evans, W. J.; Peterson, T. T.; Rausch, M. D.; Hunter, W. E.; Zhang, H.; Atwood, J. L. *Organometallics* **1985**, *4*, 554. (b) Evans, W. J.; Keyer, R. A.; Ziller, J. W. *Organometallics* **1993**, *12*, 2618.

(37) Evans, W. J.; Bloom, I.; Hunter, W. E.; Atwood, J. L. *Organometallics* **1983**, *2*, 709–714.

(38) Nolan, S. P.; Stern, D.; Marks, T. J. *J. Am. Chem. Soc.* **1989**, *111*, 7844–7853.

(39) Evans, W. J.; Ulibarri, T. A.; Ziller, J. W. *Organometallics* **1991**, *10*, 134–142.

(E = P, As). Both **1** and **2** react immediately with THF to form donor–acceptor adducts which are spectroscopically identical to the products obtained when reaction 5 is repeated using (C₅Me₅)₂Sm(THF)₂ as shown in eq 6. This reaction can



be conducted equally well in either THF or nonpolar solvents such as hexane, benzene, and toluene. However, in light of the further reactivity of **3** and **4** with THF (see below), the nonpolar solvents are preferred. Both **3** and **4** are obtained as dark green-brown powders which have lower solubility in common organic solvents than their THF-free analogs. The THF in **3** and **4** can be partially removed under vacuum, so samples of both compounds exhibit ¹H NMR spectra that are dependent on the amount of coordinated solvent removed during workup.⁴⁰ Resonances for the aromatic rings and the C₅Me₅ ligands move consistently downfield with increasing amounts of THF, reaching limiting values in the presence of an additional 1 equiv of THF. Attempts to completely remove the THF from **3** and **4** to form the unsolvated compounds **1** and **2**, respectively, were only partly successful. Heating **3** at 65 °C for 12 h under high vacuum produced a mixture of the solvent-free compound **1** and a decomposition product **5** (see below). Similar treatment of **4** gave a mixture of partially desolvated **4**, (C₅Me₅)₂Sm(AsPh₂)(THF)_x (x < 1), and an analogous decomposition product, **6**.

Structures of (C₅Me₅)₂Sm(AsPh₂), **2, and (C₅Me₅)₂Sm(AsPh₂)(THF), **4**.** Since there are currently no structural data available for Sm–As bonds and only one example of a Ln–As bonded compound in the literature,³⁵ an X-ray structural determination on **2** was performed. Structural data were also obtained on **4** for comparison with the unusual features in **2**. Selected interatomic distances and angles are given in Tables 3 and 4, and the structures of **2** and **4** are shown in Figures 1 and 2. **2** crystallizes with two independent, but chemically equivalent, molecules in the asymmetric unit, along with one hexane solvent molecule for every four molecules of **2**. The structure consists of discrete monomeric units with no unusual intermolecular contacts, which is consistent with the monomeric solution molecular weight data. **4** also crystallizes as a monomer as expected.

While there is no indication in the solid state of aggregation through bridging arsenido groups for **2**, several aspects of the data suggest an increase in coordination number through intramolecular interactions as shown in Figure 1. Both arsenic atoms in the independent molecules of **2** are located asymmetrically between the C₅Me₅ rings, as shown by the difference in (ring centroid)–Sm–As angles (117.3 vs 100.5° and 119.1 vs 100.2° for molecule 1 and molecule 2, respectively). The arsenic is also asymmetrically located with respect to the plane determined by the two ring centroids and Sm as illustrated in Figure 3. As(1) is 1.45 Å out of this plane, As(2) is displaced by 1.38 Å, and the angles between the Sm–As vectors and these planes are 29.2° [Sm(1)–As(1)] and 27.6° [Sm(2)–As(2)]. Alternatively, this asymmetry can be described in terms of the deviation of the Sm atoms from the plane formed by arsenic and the ring centroids [Sm(1) 0.35 Å, Sm(2) 0.34 Å]. The arsenic atom in **4** is also located off center (1.76 Å) from the (ring centroid)–Sm–(ring centroid) plane, but this is not unusual

(40) For a related example, see: Evans, W. J.; Drummond, D. K.; Grate, J. W.; Zhang, H.; Atwood, J. L. *J. Am. Chem. Soc.* **1987**, *109*, 3928.

Table 3. Selected Interatomic Distances (Å) and Interatomic Angles (deg) in $2 \cdot 1/4 C_6H_{14}$, $(C_5Me_5)_2Sm(AsPh_2) \cdot 1/4 C_6H_{14}^a$

molecule 1		molecule 2	
Sm(1)–As(1)	2.973(3)	Sm(2)–As(2)	2.966(3)
Sm(1)–Cnt(1)	2.413	Sm(2)–Cnt(3)	2.423
Sm(1)–Cnt(2)	2.423	Sm(2)–Cnt(4)	2.407
As(1)–C(26)	1.911(19)	As(2)–C(64)	1.965(18)
As(1)–C(32)	1.919(20)	As(2)–C(58)	1.990(18)
Sm(1)–C(31)	2.901	Sm(2)–C(59)	2.967
Sm(1)–C(32)	3.031	Sm(2)–C(64)	3.117
Sm(1)–C(1)	2.702(19)	Sm(2)–C(33)	2.698(19)
Sm(1)–C(3)	2.694(19)	Sm(2)–C(35)	2.677(21)
Sm(1)–C(5)	2.689(21)	Sm(2)–C(37)	2.693(19)
Sm(1)–C(7)	2.687(17)	Sm(2)–C(39)	2.778(19)
Sm(1)–C(9)	2.736(20)	Sm(2)–C(41)	2.674(19)
Sm(1)–C(11)	2.668(20)	Sm(2)–C(43)	2.663(21)
Sm(1)–C(13)	2.682(19)	Sm(2)–C(45)	2.655(22)
Sm(1)–C(15)	2.751(18)	Sm(2)–C(47)	2.722(22)
Sm(1)–C(17)	2.720(20)	Sm(2)–C(49)	2.680(20)
Sm(1)–C(19)	2.665(19)	Sm(2)–C(51)	2.719(21)
Cnt(1)–Sm(1)–Cnt(2)	136.3	Cnt(3)–Sm(2)–Cnt(4)	135.1
Cnt(1)–Sm(1)–As(1)	117.3	Cnt(3)–Sm(2)–As(2)	119.1
Cnt(2)–Sm(1)–As(1)	100.5	Cnt(4)–Sm(2)–As(2)	100.2
Sm(1)–As(1)–C(26)	118.8(5)	Sm(2)–As(2)–C(58)	118.5(6)
Sm(1)–As(1)–C(32)	73.0(6)	Sm(2)–As(2)–C(64)	75.4(5)
C(26)–As(1)–C(32)	104.3(8)	C(58)–As(2)–C(64)	104.9(8)
C(31)–C(32)–As(1)	115.0(15)	C(59)–C(64)–As(2)	113.1(13)
C(27)–C(32)–As(1)	129.0(16)	C(63)–C(64)–As(2)	128.8(15)
C(21)–C(26)–As(1)	119.8(14)	C(57)–C(58)–As(2)	117.3(15)
C(25)–C(26)–As(1)	125.9(14)	C(53)–C(58)–As(2)	120.5(14)

^a Cnt(1) is the centroid of the C(1)–C(3)–C(5)–C(7)–C(9) ring. Cnt(2) is the centroid of the C(11)–C(13)–C(15)–C(17)–C(19) ring. Cnt(3) is the centroid of the C(33)–C(35)–C(37)–C(39)–C(41) ring. Cnt(4) is the centroid of the C(43)–C(45)–C(47)–C(49)–C(51) ring.

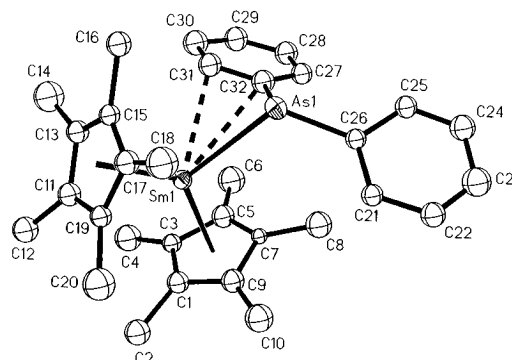
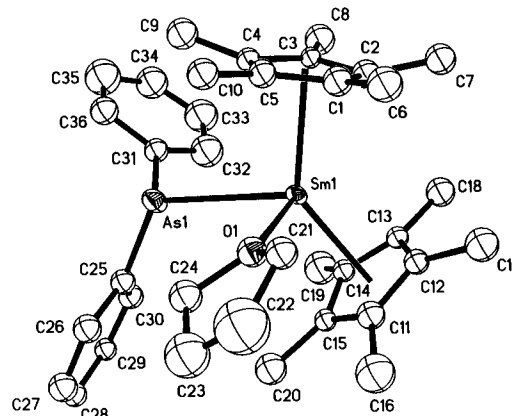
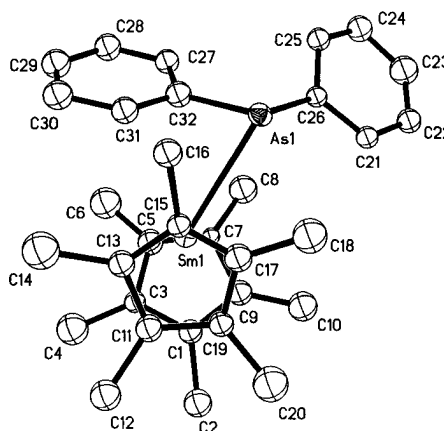
Table 4. Selected Interatomic Distances (Å) and Interatomic Angles (deg) in **4**, $(C_5Me_5)_2Sm(AsPh_2)(THF)^a$

Sm(1)–As(1)	3.049(3)	Cnt(1)–Sm(1)–Cnt(2)	136.4
Sm(1)–O(1)	2.471(15)	Cnt(1)–Sm(1)–As(1)	100.5
Sm(1)–Cnt(1)	2.464	Cnt(1)–Sm(1)–O(1)	103.3
Sm(1)–Cnt(2)	2.425	Cnt(2)–Sm(1)–As(1)	114.7
Sm(1)–C(1)	2.711(24)	Cnt(2)–Sm(1)–O(1)	102.4
Sm(1)–C(2)	2.697(24)	As(1)–Sm(1)–O(1)	88.8(3)
Sm(1)–C(3)	2.788(22)	Sm(1)–As(1)–C(25)	120.8(6)
Sm(1)–C(4)	2.772(22)	Sm(1)–As(1)–C(31)	109.1(6)
Sm(1)–C(5)	2.737(23)	C(25)–As(1)–C(31)	96.9(9)
Sm(1)–C(11)	2.728(23)	C(32)–C(31)–As(1)	122.6(16)
Sm(1)–C(12)	2.687(20)	C(36)–C(31)–As(1)	117.2(16)
Sm(1)–C(13)	2.650(21)	C(30)–C(25)–As(1)	115.9(16)
Sm(1)–C(14)	2.694(21)	C(32)–C(31)–As(1)	126.4(18)
Sm(1)–C(15)	2.738(21)		

^a Cnt(1) is the centroid of the C(1)–C(5) ring. Cnt(2) is the centroid of the C(11)–C(15) ring.

considering the presence of the additional THF ligand in the coordination sphere.

Examination of the geometry about the arsenic in **2** shows considerable deviation from either an ideal pyramidal or planar arrangement. The sum of the angles averages 297.4° and the C(ipso)–As–C(ipso) angles are 104.3(8)°–104.9(8). The Sm–As–C(ipso) angles are divided into two distinctly different sets: one group has values close to a planar arrangement [Sm(1)–As(1)–C(26) 118.8(5)° and Sm(2)–As(2)–C(58) 118.5(6)°], and the remaining set is far more acute [Sm(1)–As(1)–C(32) 73.0(6)° and Sm(2)–As(2)–C(64) 75.4(6)°]. Both narrow angles are associated with an *o*-carbon on the side of the ring closer to the samarium, which results in one ring being

**Figure 1.** Thermal ellipsoid plot of $(C_5Me_5)_2Sm(AsPh_2)$, **2**, with ellipsoids drawn at the 50% probability level.**Figure 2.** Thermal ellipsoid plot of $(C_5Me_5)_2Sm(AsPh_2)(THF)$, **4**, with ellipsoids drawn at the 50% probability level.**Figure 3.** Top view of $(C_5Me_5)_2Sm(AsPh_2)$, **2**.

tipped toward the metal in each of the molecules in the unit cell. In each of these tilted phenyl rings, one C(ortho)–C(ipso)–As angle [C(31)–C(32)–As(1) 115.0(15)°, C(59)–C(64)–As(2) 113.1(13)°] is considerably smaller than that on the opposite side of the ring [C(27)–C(32)–As(1) 129.0(16)°, C(63)–C(64)–As(2) 128.8(15)°]. In contrast, the difference between proximal and distal C(ortho)–C(ipso)–As angles observed in the adjacent phenyl rings [C(21)–C(26)–As(1) 119.8(14)°, C(57)–C(58)–As(2) 117.3(15)° vs C(25)–C(26)–As(1) 125.9(14)°, C(53)–C(58)–As(2) 120.5(14)°] is much less dramatic.

In comparison, the geometry around arsenic in $(C_5Me_5)_2Sm(AsPh_2)(THF)$ is distinctly pyramidal (sum of angles = 326.8°) and there is no overt bending of the As–C(ipso) bond toward the samarium. The Sm(1)–As(1)–C(31) angle of 109.1(6)° is perfectly regular, and the more obtuse Sm(1)–As(1)–C(31) angle to the aromatic ring nearer the THF ligand is correspond-

ingly opened to 120.8(6)°. Unlike **2**, there is no trend apparent in the C(ortho)–C(ipso)–As angles [C(32)–C(31)–As(1) 122.6(16)°, C(36)–C(31)–As(1) 117.2(16)°, C(30)–C(25)–As(1) 115.9(16)°, C(32)–C(31)–As(1) 126.4(18)°] based on the proximity of the *o*-carbon to the samarium, nor is the difference between the proximal and distal sides of the phenyl ring as pronounced as in **2**.

The result of the distortions in geometry about arsenic in **2** is that one phenyl ring is oriented toward the samarium center, with the possibility of an η^2 -interaction involving the ipso- and *o*-carbons. The shortest interatomic distances are to the *o*-carbons [Sm(1)–C(31) 2.901 Å, Sm(2)–C(59) 2.967 Å]. The samarium–ipso-carbon distances are longer [Sm(1)–C(32) 3.031 Å, Sm(2)–C(64) 3.117 Å]. In contrast, in **4** the shortest Sm···C(phenyl) distance is 4.13 Å.

In the past, when interactions of this type have been observed in organolanthanide complexes,⁴¹ a measure of their strength has been estimated by comparing the distance of the metal to the carbon in question with the metal–cyclopentadienyl carbon distance. For example, in the styrene complex, [(C₅Me₅)₂Sm]₂(μ -PhCHCH₂),⁴¹ a 2.772(17) Å Sm–C(ortho phenyl) distance is observed, which is equivalent to the 2.792(36) Å Sm–C(cyclopentadienyl) average. Since the Sm–C(cyclopentadienyl) distances in **2** are 2.665(19)–2.778(19) Å, the above secondary Sm–C(phenyl) interactions are outside the range consistent with a strong bonding interaction. However, the Sm–C(ortho phenyl) distances are comparable to the long-range interactions clearly extant in molecules like (C₅Me₅)₂Yb(MeC≡CMe),⁴² (C₅Me₅)₂Yb(μ -H₂C=CH₂)Pt(PPh₃)₂,⁴³ and (C₅Me₅)₂Sm(μ -C₅H₅)Sm(C₅Me₅)₂.⁴⁴ All of these structural observations, together with the features from the ¹H NMR spectrum (see above), support the existence of a weak interaction between the samarium and one phenyl ring in each diphenylarsenido ligand, in accordance with the expected electrophilicity of the formally seven-coordinate samarium center.

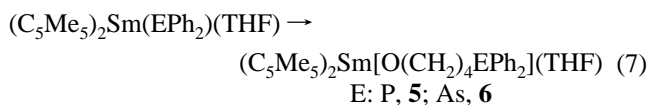
The extent of this interaction can also be evaluated by examining the structural parameters of the (C₅Me₅)₂Sm units in **2** and **4**, since a formally seven-coordinate **2** would be expected to have smaller Sm–C(C₅Me₅) distances than those in formally eight-coordinate **4**.⁴⁵ The fact that the 2.665(19)–2.778(19) Å Sm–C(C₅Me₅) distances in unsolvated **2** are indistinguishable from the analogous 2.650(21)–2.788(22) Å values in solvated **4** is consistent with **2** having an effective coordination number greater than 7. The 135.7° average (ring centroid)–Sm–(ring centroid) angle in **2** is also equivalent to the 136.4° angle in **4**.

However, the 3.049(3) Å Sm–As bond in eight-coordinate (C₅Me₅)₂Sm(AsPh₂)(THF) is about 0.08 Å longer than the 2.966(3) and 2.973(3) Å distances in **2**, which suggests that the extra phenyl coordination in **2** is not fully equivalent to another ligand such as THF. In **4**, THF approaches Sm with a Sm–O(THF) distance of 2.471(15) Å, which is typical.⁴⁵

The Sm–As bonds in both **2** and **4** are significantly longer (0.031–0.077 Å) than the 2.870(2) and 2.895(2) Å Lu–As bonds of (C₅H₅)₂Lu(μ -AsPh₂)₂Li(Me₂NCH₂CH₂NMe₂),³⁵ the only other structurally characterized lanthanide arsenic complex, even when the difference in ionic radius is taken into account. The difference between the extremes of the error limits is only 0.013 Å, but terminal lengths are typically shorter than bridging

distances. This elongation may be due to the increased steric demand of the C₅Me₅ ligand as compared to C₅H₅ in the Lu compound.

THF Ring Opening by (C₅Me₅)₂Sm(EPh₂)(THF) Compounds. In contrast to **1** and **2**, compounds **3** and **4** are not stable and undergo a further reaction involving the ring opening of the coordinated THF. As shown in eq 7, EPh₂-substituted



butoxide complexes **5** and **6** result. This ring opening occurs over a period of days at room temperature in benzene, toluene, hexane, or THF. (C₅Me₅)₂Sm[O(CH₂)₄AsPh₂](THF) can be produced on a preparative scale by heating **4** in refluxing THF for 16 h. These reactions go to completion in the presence of just 2 equiv of THF, although the reaction is slower than in neat THF. **5** and **6** also form over a period of several weeks in the solid state when stored at ambient temperature in an inert-atmosphere glovebox containing THF. Ring opening to form a substituted butoxide ligand is further observed when samples of **3** and **4** are heated under vacuum (see above). The presence of both desolvated species as well as **3** and **4** shows that loss of THF from the complexes is accompanied by nucleophilic attack on THF, which must, of necessity, be intramolecular under these conditions. This transformation is remarkable in that the ring opening reaction, which requires THF, is competitive with the loss of THF from the inner coordination sphere, even under vacuum where such loss is irreversible.

Structure of (C₅Me₅)₂Sm[O(CH₂)₄AsPh₂](THF), **6.** Compounds **5** and **6** were first identified by the distinctive appearance of the butoxide ligand in the ¹H NMR spectrum and by comparison with spectral data for the related compounds (C₅Me₅)₂Sm[O(CH₂)₃CH₃](THF),³⁹ (C₅Me₅)₂Ln[O(CH₂)₄C₅Me₅](THF) (Ln = Sm, La, Nd, Tm, Lu),^{46,47} and {(C₅H₅)₂Lu[μ -O(CH₂)₄PPh₂]}₂.⁴⁸ Where structural information is available for these compounds, the alkoxide ligands function as simple terminal or dinuclear bridging ligands with no further metal–ligand interactions. In the case of compounds **5** and **6**, however, the possibility exists for secondary ligation from the EPh₂ terminus to form a seven-membered Sm–O(CH₂)₄E cycle. To explore this possibility, an X-ray structural determination was carried out on **6**, which confirmed the presence of the THF-derived ligand suggested by the spectral data (Figure 4). Selected bond lengths and angles are given in Table 5.

The molecular structure of (C₅Me₅)₂Sm[O(CH₂)₄AsPh₂](THF) shows an eight-coordinate geometry about the samarium with an approximately tetrahedral arrangement of cyclopentadienyl ring centroids and oxygen atoms. The angle between the (ring centroid)–Sm–(ring centroid) and O–Sm–O planes is 89.9°. The butoxide ligand coordinates in a terminal fashion, and there is no interaction between the diphenylarsenido ligand and the samarium. Overall, the (C₅Me₅)₂SmO₂ geometry for the complex is quite similar to that of (C₅Me₅)₂Sm[O(CH₂)₄C₅Me₅](THF), with the corresponding Sm–O(butoxide), Sm–O(THF), and average Sm–C(ring carbon) distances in both compounds within experimental error of each other. The distinct trend toward linearity in the 165.2(7)° Sm–O–C bond angle in (C₅Me₅)₂Sm[O(CH₂)₄C₅Me₅](THF)⁴⁶ (and other lanthanide

(41) Evans, W. J.; Ulibarri, T. A.; Ziller, J. W. *J. Am. Chem. Soc.* **1990**, *112*, 219.

(42) Burns, C. J.; Andersen, R. A. *J. Am. Chem. Soc.* **1987**, *109*, 941.

(43) Burns, C. J.; Andersen, R. A. *J. Am. Chem. Soc.* **1987**, *109*, 915.

(44) Evans, W. J.; Ulibarri, T. A. *J. Am. Chem. Soc.* **1987**, *109*, 4292.

(45) Evans, W. J.; Foster, S. E. *J. Organomet. Chem.* **1992**, *433*, 79.

(46) Evans, W. J.; Ulibarri, T. A.; Chamberlain, L. R.; Ziller, J. W.; Alvarez, D. *Organometallics* **1990**, *9*, 2124–2130.

(47) Schumann, H.; Glanz, M.; Hemling, H.; Gorlitz, F. H. *J. Organomet. Chem.* **1993**, *462*, 155.

(48) Schumann, H.; Palamidis, E.; Loebel, J. *J. Organomet. Chem.* **1990**, *384*, C49.

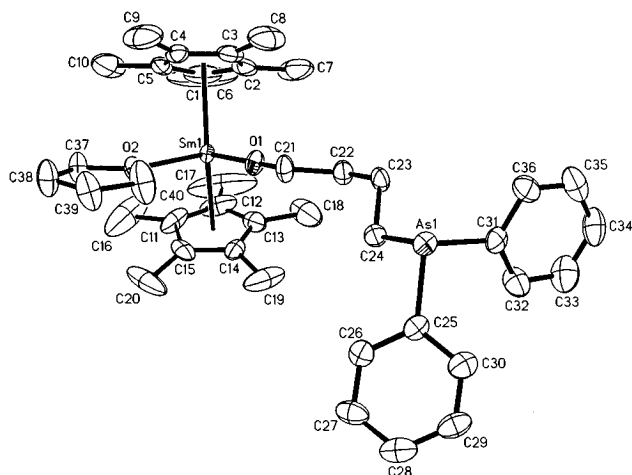


Figure 4. Thermal ellipsoid plot of $(C_5Me_5)_2Sm[O(CH_2)_4AsPh_2](THF)$, **6**, with ellipsoids drawn at the 50% probability level.

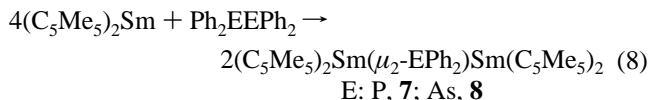
Table 5. Selected Interatomic Distances (Å) and Interatomic Angles (deg) in **6**, $(C_5Me_5)_2Sm[O(CH_2)_4AsPh_2](THF)^a$

Sm(1)–O(1)	2.085(5)	Cnt(1)–Sm(1)–Cnt(2)	136.0
Sm(1)–O(2)	2.475(5)	Sm(1)–O(1)–C(21)	175.4(4)
Sm(1)–Cnt(1)	2.478	O(1)–Sm(1)–O(2)	85.3(2)
Sm(1)–Cnt(2)	2.479	Cnt(1)–Sm(1)–O(1)	107.1
Sm(1)–C(1)	2.754(9)	Cnt(1)–Sm(1)–O(2)	107.2
Sm(1)–C(2)	2.699(9)	Cnt(2)–Sm(1)–O(1)	104.8
Sm(1)–C(3)	2.729(8)	Cnt(2)–Sm(1)–O(2)	104.7
Sm(1)–C(4)	2.760(7)	C(24)–As(1)–C(25)	98.3(3)
Sm(1)–C(5)	2.790(9)	C(24)–As(1)–C(31)	97.9(3)
Sm(1)–C(11)	2.749(10)	C(25)–As(1)–C(31)	101.7(3)
Sm(1)–C(12)	2.752(9)		
Sm(1)–C(13)	2.731(8)		
Sm(1)–C(14)	2.742(7)		
Sm(1)–C(15)	2.767(8)		

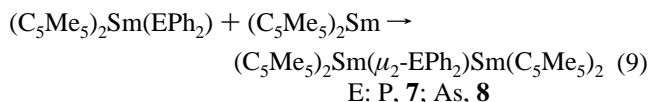
^a Cnt(1) is the centroid of the C(1)–C(5) ring. Cnt(2) is the centroid of the C(11)–C(15) ring.

alkoxides)⁴⁹ is also followed in **6**, where the Sm(1)–O(1)–C(21) angle reaches an even larger value of 175.4(4)°.

Reaction of $(C_5Me_5)_2Sm$ with $(C_5Me_5)_2Sm(EPh_2)$ (E = P, As) To Form Mixed-Valent Products. Formation of Sm–EPh₂ complexes from Ph₂EPh₂ precursors is consistent with the relative E–E and E–C bond strengths in these compounds. In efforts to cleave the E–C bonds in these compounds, **1** and **2** were treated with additional $(C_5Me_5)_2Sm$; i.e., reaction 5 was run with a 4:1 stoichiometry as shown in eq 8. Alternatively,



isolated $(C_5Me_5)_2Sm(EPh_2)$ can be reacted with $(C_5Me_5)_2Sm$ in a 1:1 ratio as shown in eq 9 to form products that are



spectroscopically the same as those formed in eq 8. On the basis of ¹H NMR data, a new compound is formed in both cases, but only for E = P has a new product, **7**, been isolated and

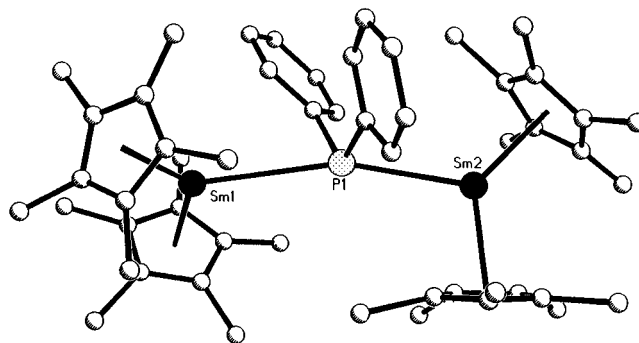


Figure 5. Structure of $(C_5Me_5)_2Sm(\mu-PPh_2)Sm(C_5Me_5)_2$, **7**.

definitively characterized by X-ray crystallography⁵⁰ (Figure 5). The corresponding arsenic product, **8** (E = As), is unstable, showing signs of decomposition within 15 min of synthesis, and was characterized only in solution by ¹H NMR spectroscopy. Neither product results from E–C cleavage; each results instead from coordination of $(C_5Me_5)_2Sm$ to the lone pair of electrons of the respective pnictide. It is noteworthy that these “ $(C_5Me_5)_2Sm$ ” complexation reactions do not occur when $(C_5Me_5)_2Sm(THF)_2$ is substituted for $(C_5Me_5)_2Sm$. In other words, $(C_5Me_5)_2SmEPh_2(THF)$ compounds **3** and **4** do not undergo any further reaction in the presence of additional equivalents of $(C_5Me_5)_2Sm(THF)_2$. The ¹H NMR spectra of the reaction mixtures are a simple superposition of the two components.

The ¹³C NMR and magnetic data for **7** give an indication of the electronic structure of this formally mixed-oxidation-state Sm(II,III) compound. Resonances for the C_5Me_5 ring and methyl carbons in the ¹³C NMR spectra of compounds **1–6** fall in the ranges 113–118 and 18–20 ppm, respectively, as is common for trivalent (pentamethylcyclopentadienyl)samarium complexes. In contrast, the methyl carbons in **7** are observed at 57.3 ppm and the ring carbon resonance appears at 17.8 ppm. These unusual positions do not resemble those found in typical divalent pentamethylcyclopentadienyl compounds but rather lie between the values observed for strictly divalent and trivalent complexes,^{1b,51} as is observed for a related mixed-valent complex $(C_5Me_5)_2Sm(\mu-C_5H_5)Sm(C_5Me_5)_2$.⁴⁹

Similarly, the room-temperature molar magnetic susceptibility of $(C_5Me_5)_2Sm(\mu_2-PPh_2)Sm(C_5Me_5)_2$ measured in benzene solution⁵² is 2560×10^{-6} cgsu, giving an effective magnetic moment per samarium of 2.45 μ_B . The former value is close to the average of the susceptibilities per metal center for the individual components $(C_5Me_5)_2Sm$, 5050×10^{-6} cgsu,²¹ and $(C_5Me_5)_2Sm(PPh_2)$, 425×10^{-6} cgsu. The magnetic data alone indicate that **7** is a class I mixed-valence system⁵³ where the two metals exist in distinct oxidation states. However, the single resonance in the ¹H NMR spectrum and the unusual shifts for the cyclopentadienyl ligands in the ¹³C NMR spectrum are indicative of a single, or perhaps averaged, environment. Together, these data suggest that in solution there is some degree of delocalization mediated through the bridging diphenylphosphido unit, allowing for a change between the Sm(II) and Sm(III) oxidation states that is rapid on the NMR time scale. Irrespective of the actual valence description, the availability of the divalent $(C_5Me_5)_2Sm$ moiety in **7** for further reactivity is

(50) Several attempts were made to obtain precise metrical data for crystals of **7**, but the data were not of sufficient quality to yield any information other than atom connectivity.

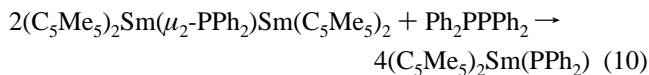
(51) Evans, W. J.; Ulibarri, T. A. *J. Am. Chem. Soc.* **1987**, *109*, 4292.

(52) Evans, D. F. *J. Chem. Soc.* **1959**, 2003. Beconsall, J. K. *Mol. Phys.* **1968**, *15*, 129.

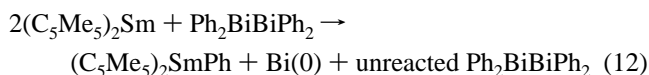
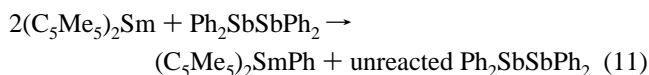
(53) Robin, M. B.; Day, P. *Adv. Inorg. Chem. Radiochem.* **1967**, *10*, 247.

(49) (a) Evans, W. J.; Sollberger, M. S.; Hanusa, T. P. *J. Am. Chem. Soc.* **1988**, *110*, 1841. (b) Evans, W. J.; Hanusa, T. P.; Levan, K. R. *Inorg. Chim. Acta* **1985**, *110*, 191 and references therein.

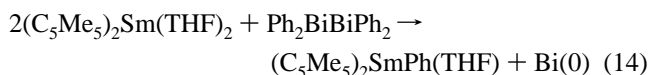
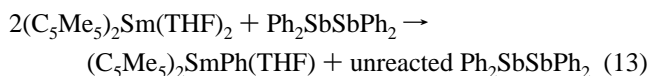
evidenced by the P–P bond cleavage of Ph_2PPPh_2 and its conversion back to $(\text{C}_5\text{Me}_5)_2\text{Sm}(\text{PPh}_2)$, eq 10.



Reactions of $(\text{C}_5\text{Me}_5)_2\text{Sm}$ and $(\text{C}_5\text{Me}_5)_2\text{Sm}(\text{THF})_2$ with $\text{Ph}_2\text{SbSbPh}_2$ and $\text{Ph}_2\text{BiBiPh}_2$. In contrast to the phosphorus and arsenic systems described above, eqs 5 and 6, the analogous reactions with antimony and bismuth do not simply lead to cleavage of the element–element bond. In each case, E–C bond cleavage occurs with $(\text{C}_5\text{Me}_5)_2\text{Sm}$, as evidenced by the appearance of $(\text{C}_5\text{Me}_5)_2\text{SmPh}$, eqs 11 and 12. The reactions



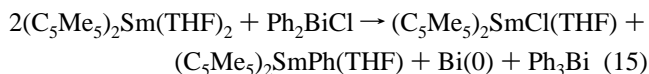
with $(\text{C}_5\text{Me}_5)_2\text{Sm}(\text{THF})_2$ mirror those of the THF-free reactions, except that $(\text{C}_5\text{Me}_5)_2\text{SmPh}(\text{THF})$ is produced, eqs 13 and 14.



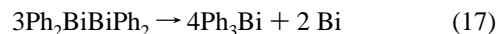
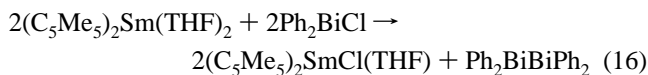
With these Ph_2EPh_2 substrates, no $(\text{E}_2)^{2-}$ or $(\text{E}_3)^{3-}$ products are observed. Only elemental bismuth and antimony are obtained. The bismuth reactions readily deposit elemental bismuth, but the antimony reactions are curious in that elemental antimony does not appear until the reactions have run for 1–3 days. Intermediate products have been neither isolable nor identifiable by ^1H NMR spectroscopy. Neither variation in the solvent from hexane to arenes to THF nor low temperature reactions have yielded any other compounds.

Reactions of $(\text{C}_5\text{Me}_5)_2\text{Sm}$ and $(\text{C}_5\text{Me}_5)_2\text{Sm}(\text{THF})_2$ with Ph_2BiX . Since the reactivity of Ph_3Bi to form $[(\text{C}_5\text{Me}_5)_2\text{Sm}]_2(\mu\text{-}\eta^2\text{:}\eta^2\text{-Bi}_2)$ was found to be unique in the group 15 Ph_3E and Ph_2EPh_2 compounds investigated, the reactions of Ph_2BiCl with $(\text{C}_5\text{Me}_5)_2\text{Sm}$ and $(\text{C}_5\text{Me}_5)_2\text{Sm}(\text{THF})_2$ were examined to see if they would parallel that of Ph_3Bi or $\text{Ph}_2\text{BiBiPh}_2$. Halide abstraction was expected to form $(\text{C}_5\text{Me}_5)_2\text{SmCl}^{40}$ and $(\text{C}_5\text{Me}_5)_2\text{SmCl}(\text{THF})$,⁵⁴ respectively. This would leave a Ph_2Bi moiety which could couple to $\text{Ph}_2\text{BiBiPh}_2$ or react with $(\text{C}_5\text{Me}_5)_2\text{Sm}(\text{THF})_x$ to form $(\text{C}_5\text{Me}_5)_2\text{Sm}(\text{BiPh}_2)(\text{THF})_x$. Either pathway would lead to the formation of Sm–Bi or Bi–Bi bonds necessary for the assembly of $[(\text{C}_5\text{Me}_5)_2\text{Sm}]_2(\mu\text{-}\eta^2\text{:}\eta^2\text{-Bi}_2)$.

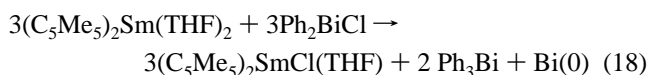
Reaction of $(\text{C}_5\text{Me}_5)_2\text{Sm}(\text{THF})_2$ with a 2:1 Sm/Bi ratio as shown in eq 15 gives a variety of products resulting from both



Bi–Cl and Bi–Ph cleavage, as well as small amounts of products consistent with limited reductive coupling of Ph_2BiCl (see below). The 1:1 reaction is more selective and leads only to Bi–Cl cleavage, eq 16. Coupling of Ph_2BiCl to form $\text{Ph}_2\text{BiBiPh}_2$ is implied by the presence of $\text{Bi}(0)$ and Ph_3Bi as products of dibismuthine disproportionation, eq 17. $\text{Bi}(0)$ is



quantitatively recovered according to the net overall reaction shown in eq 18. Reactions conducted with $(\text{C}_5\text{Me}_5)_2\text{Sm}$ in place



of $(\text{C}_5\text{Me}_5)_2\text{Sm}(\text{THF})_2$ proceed analogously to eqs 15 and 16, except that the THF-free compounds $(\text{C}_5\text{Me}_5)_2\text{SmCl}$ and $(\text{C}_5\text{Me}_5)_2\text{SmPh}$ are formed. This chemistry is reminiscent of that with alkali metals and Ph_2BiCl . A 1:1 ratio of Na: Ph_2BiCl in liquid ammonia leads to reductive coupling and the formation of $\text{Ph}_2\text{BiBiPh}_2$.⁵⁵ Excess alkali metal effects cleavage of the Bi–Bi bond and affords $\text{Bi}(0)$ and Ph_3Bi .⁵⁶

Conclusion

$(\text{C}_5\text{Me}_5)_2\text{Sm}$ and $(\text{C}_5\text{Me}_5)_2\text{Sm}(\text{THF})_2$ react with aryl-substituted group 15 compounds by three modes: coordination, E–C cleavage, and E–E cleavage. E–C cleavage is most common for the heavier congeners, which have weaker E–C bonds. Hence, $(\text{C}_5\text{Me}_5)_2\text{SmPh}$ products are found in reactions with Sb and Bi but not with P and As. E–E cleavage occurs with all of the systems studied: P, As, Sb, and Bi. For the lighter congeners with stronger E–C bonds, the E–E cleavage products are isolated as the EPh_2 complexes $(\text{C}_5\text{Me}_5)_2\text{Sm}(\text{PPh}_2)$ and $(\text{C}_5\text{Me}_5)_2\text{Sm}(\text{AsPh}_2)$. The THF adducts display further chemistry and provide a system in which THF coordination and ring opening can be separately defined. The base-free complexes interact with additional $(\text{C}_5\text{Me}_5)_2\text{Sm}$ to form mixed-valent compounds. Reaction of $(\text{C}_5\text{Me}_5)_2\text{Sm}$ with Ph_3Bi appears to be a rather special case, since it is the only one in which the $(\text{E}_2)^{2-}$ ion is isolated. Hence, the dibismuth complex $[(\text{C}_5\text{Me}_5)_2\text{Sm}]_2(\mu\text{-}\eta^2\text{:}\eta^2\text{-Bi}_2)$ is accessible from neither $\text{Ph}_2\text{BiBiPh}_2$ nor Ph_2BiCl and the only organosamarium products of reactions with other Ph_3E complexes are E–C(phenyl) cleavage products.

The complexes $(\text{C}_5\text{Me}_5)_2\text{Sm}(\text{AsPh}_2)$, **2**, and $(\text{C}_5\text{Me}_5)_2\text{Sm}(\text{AsPh}_2)(\text{THF})$, **4**, constitute an interesting pair of compounds which show the flexibility of the $(\text{C}_5\text{Me}_5)_2\text{Sm}$ unit to stabilize different ligand systems. The isolation and structural characterization of the lower coordinate **2** are possible, although there is clearly room for the addition of THF to form **4**. The isolation of **4** indicates that this typical eight-coordinate structure is possible even with ligands as large as AsPh_2 . However, **4** can be desolvated under vacuum and can engage in THF ring-opening reactivity. Studies directed toward exploiting this unusual balance of steric saturation are in progress.

Acknowledgment. We thank the National Science Foundation for support for this research.

Supporting Information Available: Tables of crystal data, positional parameters, bond distances and angles, and thermal parameters (35 pages). Ordering information is given on any current masthead page.

IC951627Z

(54) Evans, W. J.; Grate, J. W.; Levan, K. R.; Bloom, I.; Peterson, T. T.; Doedens, R. J.; Zhang, H.; Atwood, J. L. *Inorg. Chem.* **1986**, *25*, 3614.

(55) (a) Calderazzo, F.; Morvillo, A.; Pelizzi, G.; Poli, R. *J. Chem. Soc., Chem. Commun.* **1983**, 507. (b) Calderazzo, F.; Poli, R.; Pelizzi, G. *J. Chem. Soc., Dalton Trans.* **1984**, 2365. (c) Ashe, A. J.; Ludwig, E. C.; Oleksyszyn, J. *Organometallics* **1983**, *2*, 1859. (d) Fischer, E. O.; Reitmeier, R. Z. *Naturforsch., B* **1983**, *38*, 582. (e) Breunig, H. J.; Müller, D. *J. Organomet. Chem.* **1983**, *253*, C21.

(56) Gilman, H.; Yablunsky, H. *J. Am. Chem. Soc.* **1941**, *63*, 212.